Title
Influence of Dissolved O2 in Organic Solvents on CuOEP Supramolecular Self-Assembly on Graphite.

Journal
Langmuir : the ACS journal of surfaces and colloids, 32(22)

ISSN
0743-7463

Authors
Hao, Yibo
Weatherup, Robert S
Eren, Baran
et al.

Publication Date
2016-06-01

DOI
10.1021/acs.langmuir.6b01580

Peer reviewed

The Influence of Dissolved O_2 in Organic Solvents on CuOEP Supramolecular Self-Assembly on Graphite

Yibo Hao,†, Robert S. Weatherup,†, Baran Eren,†, Gabor A. Somorjai,‡, ¶, Miquel Salmeron,*,†,¶

† *Materials Sciences Divisions, Lawrence Berkeley National Laboratory, 1 Cyclotron Road, Berkeley, California 94720, United States,* ‡ *Department of Chemistry, University of California, Berkeley, United States,* ¶ *Department of Materials Science and Engineering, University of California, Berkeley, United States*

∗ E-mail: mbsalmeron@lbl.gov Phone: +1 510-486-6704

Keywords: CuOEP, Liquid-STM, supramolecular self-assembly, enzyme, O_2

Abstract

The supramolecular self-assembly of copper (II) octaethylporphyrin (CuOEP) and octaethyporphyrin (H_2OEP) on graphitic surfaces immersed in organic solvents (dichlorobenzene, dodecane) is studied using scanning tunneling microscopy (STM) and Raman spectroscopy. STM reveals that the self-assembled structure of CuOEP in 1,2-dichlorobenzene is significantly altered by dissolved oxygen within the solvent. Raman spectroscopy reveals that the presence of the oxygen alters the molecule-substrate interaction, which is attributed to the adsorption of oxygen on the Cu center of the CuOEP, which is facilitated by electron transfer from the graphitic surface. Such oxygen-induced changes are not observed for H_2OEP, indicating that the metal center of CuOEP plays a critical role. When the solvent is dodecane, we find that solvation effects dominate. CuOEP adsorbed on graphitic surfaces provides a model system relevant to the study of the transport and activation of oxygen by enzymes and other complexes.

1. Introduction

Porphyrin molecules assemble into quasi-two dimensional films on various substrates, as shown by scanning tunneling microscopy (STM) which has become the predominant tool for investigating their interactions with each other and with the substrate.[1-6] Most studies in the past decade have focused on the electronic properties of porphyrins relevant to various nanotechnological applications.[7-9] Metalloporphyrin (i.e. porphyrins with metallic centers) complexes are extremely important and abundant in biological systems. They constitute the active sites of many enzymes, the biological catalysts that operate in aqueous solutions at body temperature. Among them, one of the most recognizable catalytic processes is oxygen transfer in human and animal blood, with Fe-centered porphyrins in hemoglobin and myoglobin being the active sites.[10] Metalloporphyrins are also present in chlorophyll and vitamin B12 which have Mg and Co centers respectively.[10] Although there are no enzymes that have Cu-centered porphyrins as active sites, Cu centers exist in other complexes that play important roles in the transport and activation of oxygen, such as hemocyanins.[11] Because hemocyanins and other proteins cannot be readily probed with STM at the molecular level due to their structural complexity, Cu-centered porphyrins can be used as surrogates to investigate their interaction with molecular oxygen.

In most previous STM studies, porphyrins were vapor deposited onto single crystal metal substrates, which requires ultra-high vacuum conditions to keep the surfaces clean.[3-5,12] In our experiments we dissolve porphyrins in electrically nonconductive organic solutions and the porphyrin molecules form self-assembled monolayers at the solid-liquid interface between the organic solution and the basal plane of graphite through non-covalent interactions.[5,13-14] An important factor here is the length of the alkyl substituent groups of the porphyrins, where longer chains are expected to provide a stronger interaction with the graphite.[15] We used

octaethylporphyrins (OEP) in this work to achieve sufficient interaction with the graphite surface such that the arrangement of the molecules remains stable during imaging. Various experimental studies and theoretical models of the geometry and molecular conformation of metal-OEP (M-OEP) systems on graphite are available in literature[16-19]. At the solid-liquid interface, both the self-assembled geometry (lattice vectors and packing density) and molecule conformation result from an interplay of molecule-molecule, molecule-substrate, molecule-solvent, and substrate-solvent interactions. In the absence of the last two of these interactions (solvation effects), the M-OEP molecular conformation, with M = Co or Ni, is typically crown-like: Central rings lie flat on the graphitic surface while the ethyl groups point upwards.[18-19] Regarding solvation effects, alkane solvents are especially important because they have a nearly perfect lattice match with the graphitic basal plane and thereby strong van der Waals interactions, so they may compete with the porphyrins for the adsorption sites.[13]

Another important factor that may affect self-assembly of metal centered porphyrins are impurities, especially dissolved O_2. Surprisingly, not much attention has been paid to this in the literature. An exception is CoOEP,[20] where O_2 was claimed to bind to the Co centers when the molecules were supported on a graphite substrate. In this work, we study the effects of O_2 in 1,2-dichlorobenzene (DCB) and dodecane (DD). We find that dissolved O_2 changes the supramolecular self-assembly when the interaction between the metal center and the substrate is strong, as is the case for CuOEP/Graphite in DCB. For the cases where the interaction is weak, as for CuOEP/Graphite in DD or for molecules lacking the metal center (H_2OEP/ Graphite interface in DCB), O_2 impurities inside the solution do not cause significant changes in the self-assembly. Raman spectroscopy reveals that the presence of oxygen within the DCB solution alters the molecule-substrate interaction, thus supporting the model suggested by STM. Our

results not only highlight the importance of dissolved O_2, but also have a relevance to biochemistry as explained above.

2. Experimental

Solid crystals of CuOEP (Figure 1a, Sigma-Aldrich, 97% purity) and H_2OEP (Figure 1b, Sigma-Aldrich, 95% purity) were separately dissolved in DCB and DD at very low concentrations (< 0.001M). Experiments with freshly prepared solutions were performed within less than 0.5 hours of exposure to air to minimize the amount of dissolved oxygen. Oxygen treated samples were prepared by bubbling oxygen gas directly into the sample solution in a sealed bottle for 1-2 hours.

STM experiments were performed using an RHK scanner with SPM 100 control electronics. A Viton O-ring was placed on top of a highly oriented pyrolytic graphite (HOPG) substrate sealing it between two plates of the sample stage. The upper plate had a hole in its center, allowing for insertion of 3-4 droplets of the liquid to cover the HOPG surface. Since the solvents used in the present study have low vapor pressures the HOPG remained wetted by the solvents for 10-12 hours. Commercial Pt/Ir tips (Bruker PT10) were used, with the tip grounded and the bias voltage applied to the sample. Imaging parameters are indicated in the image captions. Lattice parameters of the supramolecular self-assemblies are extracted by fitting the 2D autocorrelation of the topography images. Images taken with different scan rates were analyzed to account for any contribution from thermal drift. The stated error bars correspond to the standard deviation of the parameters extracted from multiple images taken for similar samples.

Raman spectroscopy was performed using a Horiba Jobin Yvon LabRAM ARAMIS confocal Raman microscope using a 50× long working distance objective and 532 nm excitation wavelength. We use CVD-graphene[21] deposited on Cu foil (Graphene Supermarket®) and transferred onto SiO_2 (300 nm)/Si as a model system to study the charge transfer between CuOEP and graphitic surfaces. The graphene is transferred using a polymer-free method[22] that avoids any polymer residues that may influence the supramolecular self-assembly.[23] A drop of solution was placed on the surface of the sample and a glass coverslip was placed on top to produce a film of solution on top of the sample of uniform thickness. The spectral features arising from the atomically thin graphene are inherently surface sensitive allowing relatively modest changes in doping to be resolved (compared to using bulk graphite). To avoid sample dependent variations, the same location (to within ~1 μm) was illuminated in all measurements. The sample was rinsed with fresh DCB between each change of solution.

3. Results and Discussion

3.1 Solvation effects

Figure 1 shows images of the self-assembled monolayers of CuOEP and H_2OEP molecules at the HOPG-DCB interface (c and d, respectively), and at the HOPG-DD interface (in e and f, respectively) for freshly prepared samples. The CuOEP molecules in DCB assemble in a quasi-hexagonal lattice arrangement on HOPG (Figure 1c, $\Theta = 66.7 \pm 4.5°$), similar to that formed in air by NiOEP, a porphyrin with molecular structure and size similar to that of CuOEP.[12] This similarity in the self-assemblies is attributed to the weak interaction between DCB and HOPG,[24] which leads to the molecule-substrate interaction dominating. For H_2OEP in

DCB (Figure 1d), which lacks a metallic center, a quasi-orthogonal self-assembly is instead observed ($\Theta = 96.5 \pm 1.9°$). This prominent difference between the self-assemblies of CuOEP and H_2OEP molecules on HOPG under the same conditions indicates that the Cu center changes substantially the interaction with the substrate. For M-OEP molecules where the central metal atom is coplanar with the carbon ring (such as Cu, Co, Ni), theoretical studies predict the highest interaction to be through the π-system.[19] This interaction is higher for smaller separation distances produced when the ethyl groups point up in a crown-like structure.[19] Therefore, the bright contrast in (c) and (d) is attributed to the electron rich carbon rings of the OEP molecules.

The self-assembly geometries of both CuOEP and H_2OEP are very different in DD than in DCB. Because the linear alkane structure of DD has an almost perfect lattice match with HOPG,[13] its van der Waals interaction with the substrate is significant. Although DD itself could not be imaged in our STM, it most likely coadsorbs with the porphyrin molecules. A similar solvent (n-tetradecane) was previously claimed to promote the bending of the alkane chains of alkylated porphyrin molecules towards the HOPG surface,[25] which subsequently increases the separation between the central body (consisting of four carbon rings) of the porphyrin and the substrate, and thereby reduces the total interaction between the central body and substrate.[19] The results of this strong solvation effect can be seen in the STM images in Figure 1(e) and (f), where both CuOEP and H_2OEP show higher packing densities of ~0.6 molecules/nm^2 than those in DCB (~0.5 molecules/nm^2). Such an increase in packing density has been associated with a weaker molecule-substrate interaction relative to the intermolecular interactions.[17,26]

Figure 2 shows a time-series of STM images of CuOEP molecules at the DD HOPG interface. In the course of scanning, CuOEP molecules can be easily removed with the STM tip away from the scanned area towards the borders of the frame. A similar observation was also

made for H_2OEP molecules at the HOPG-DD interface. This phenomenon was never observed when DCB was used as the solvent, suggesting that the solvation effects in DD significantly weaken the molecule-substrate interaction. Furthermore, it was observed by optical microscopy (performed as part of the Raman measurements) that whilst the single layer graphene on SiO_2 remained intact for all the measurements with DCB as the solvent, when DD was instead used some graphene regions were removed from the SiO_2 surface. This is indicative of DD weakening the already weak interaction between Graphene and SiO_2. We note that a small proportion (<2 %) of the centers of the supramolecular self-assembly measured in Figure 2A,B appear to have slightly different contrasts compared to the others. Previous reports have suggested that such contrast changes may correspond to changes in the oxidation state of porphyrin molecules, related to the presence of different gas species and/or the bias voltage.[27] However we exclude this effect in this case as we see no significant change in the proportion of such centers following oxygen-bubbling, or when applying different bias voltages (V_b in the range 0.5-1.2 V). We do however see much fewer of these different contrast centers when DCB is used as the solvent. We therefore attribute them to vacancies/mobile porphyrin molecules, with their increased prevalence with DD being consistent with the lower molecule-substrate interaction observed with this solvent. We also note the samples of porphyrin molecules used are only 95-97% pure, and thus the presence of other porphyrin molecules with different metal centers or lacking metal centers may also lead to contrast changes with both DD and DCB as solvents.

3.2 Effect of dissolved oxygen

Figure 3 shows the STM images of self-assembled layers of CuOEP and H_2OEP molecules after the oxygen bubbling treatment ((a) and (b) in DCB solution; (c) and (d) in DD solution). Although the oxygen solubility of DCB and DD is not well studied in literature, similar organic

solvents (chlorobenzene and decane), were reported to have similar oxygen solubilities.[28] Significantly, the image in Figure 3a shows a different supramolecular arrangement for CuOEP than that before oxygen treatment (Figure 1c). The angle between the lattice vectors in Figure 3a (Θ = 94.9 ± 1.1°) indicates a quasi-orthogonal lattice. Clearly, the interaction with oxygen is responsible for this change. In contrast, for H_2OEP molecules lacking the metallic center, no change in geometry was observed upon oxygenation of the solvent (Figure 3b). The lattice angle (Θ = 93.4 ± 2.2°) is still very similar to that before oxygen treatment (Θ = 96.5 ± 1.9°), in Figure 1d). The STM experiments on these different supramolecular self-assemblies thus show that only the Cu centered porphyrin molecules undergo changes upon oxygenation of the DCB solvent, suggesting adsorption of O_2 on the Cu center of the CuEOP molecules. Oxygen is known to bind to many metalloporphyrins such as Fe(II)-porphyrins in nature.[29] However, unlike Fe, Cu does not typically have a +3 oxidation state, so a charge transfer to adsorbed oxygen is only possible via charge donation from the underlying graphitic substrate to Cu centers of the porphyrins. This mechanism was also recently proposed for CoOEP molecules.[20]

Figures 3c and 3d show the effects of oxygenation treatment when DD is used as the solvent. In this case however, the lattice angles in Figure 3c (Θ = 64.4 ± 2.4°) and 3d (Θ = 65.1 ± 3.7°) measured after oxygen bubbling are very similar to the lattice angles of the images in Figure 1e (Θ = 66.6 ± 2.4°) and 1f (Θ = 67.2 ± 4.6°) measured prior to oxygen treatment. Also, the intermolecular distances of both CuOEP and H_2OEP self-assembled layers (Figures 3c and 3d) remain very similar to those measured prior to oxygen treatment. For the H_2OEP layer, the preservation of the initial geometry is expected due to the lack of metallic center as described in the previous section. For CuOEP, the results can be best understood as due to the larger separation of the CuOEP self-assembled layer from the HOPG surface due to the stronger

solvation effects of DD. The resulting weaker interaction between HOPG and CuOEP hinders the charge transfer from the substrate that is needed for oxygen to bind to the Cu center. Thus for CuOEP in DD, given the weak molecule-substrate interaction, the other interactions, including solvent-substrate, molecule-molecule and molecule-solvent interactions are expected to be driving the supramolecular assembly.

3.3 Raman spectroscopy

Figure 4 summarizes the results of Raman spectroscopy measurements performed to further understand the origin of the change in the supramolecular assembly of the CuOEP molecules in DCB. Whilst both the solvent and solute molecules exhibit numerous spectral features, we focus on the graphene-related peaks as we are primarily interested in probing the graphene-solvent interface. A Lorentzian line shape is used for fitting both the G and 2D peaks of graphene and the intensity ratio I_{2D}/I_G is calculated from the ratio of the fitted peak heights. The as-transferred graphene shows the characteristic G (1588 cm^{-1}) and 2D (2682 cm^{-1}) peaks of single layer graphene (Figure 4a), with the 2D peak well fitted with a single Lorentzian of 31 cm^{-1} fwhm, and a 2D-G intensity ratio of 2.4. A negligible D-peak (expected at ~1350 cm^{-1}) confirms the high graphitic quality of the as-transferred graphene. The 2D and G peak positions indicate the graphene is initially slightly p-doped, consistent with the presence of atmospheric contaminants due to the storage of the sample in air for several days.[30] The addition of DCB leads to upshifts in both the G and 2D peak positions by 10.5 and 7.1 cm^{-1} respectively, as well as reductions in the fwhm of the G and 2D peaks to 7.4 and 27.9 cm^{-1} and the 2D-G intensity ratio to 1.2. This is predominantly attributed to the substrate-solvent interaction of the DCB with the graphene layer. When oxygen bubbled DCB is instead used, the only significant change in the Raman spectrum (Figure 4a) is a reduction in the intensity ratio between the DCB- and

graphene-related peaks, which is attributed to a thinner DCB film being sandwiched between the cover slip and graphene (i.e. unrelated to the oxygen bubbling treatment). The widths, positions and relative intensities of the graphene-related peaks remain almost identical (Figure 4b), indicating that the presence of dissolved oxygen does not significantly alter the substrate-solvent interaction.

With CuOEP dissolved in DCB that has not undergone an O_2-bubbling treatment, a clear Raman signature related to the CuOEP is observable alongside the DCB and graphene related features (Figure 4a).[31] However, when measuring a region of the SiO_2(300 nm)/Si that is not covered with graphene (not shown), the CuOEP signal is absent whilst the DCB signatures are still observed indicating that the presence of the graphitic surface is key to the supramolecular assembly of the porphyrins that we observe by STM. The adsorption of the porphyrin molecules also leads to a clear change in the graphene spectra, with the G peak slightly downshifted to 1597.9 cm^{-1} and the 2D peak slightly upshifted to 2690.5 cm^{-1}. The widths of the G and 2D peaks also increase significantly to 9.3 and 31.4 cm^{-1} fwhm respectively, and their intensity ratio reduces slightly to 1.1. For the CuOEP dissolved within DCB that has been bubbled with O_2, we see further changes in the graphene-related Raman peaks, with the G peak further downshifted to 1594.5 cm^{-1} whilst the 2D peak is now also downshifted to 2687.9 cm^{-1}. The fwhm of the G and 2D peaks are decreased to 8.0 and 27.1 cm^{-1}, whilst the 2D-G ratio drops further still to 0.87. These significant differences in the Raman spectra of the graphene before and after oxygen bubbling that are only observed with CuOEP within the DCB solution, confirm that oxygenation of the solution significantly alters the interaction of CuOEP with the graphitic surface, which is attributed to molecular oxygen adsorbed onto the Cu center of CuOEP. Notably however, ultraviolet-visible spectroscopy measurements (not shown) show no distinguishable change

following oxygenation of the solution, indicating that oxygen does not bind to CuOEP in the bulk of the solution, further supporting the conclusion that this binding is facilitated by the interaction with the graphitic surface.

We use single-layer graphene for the Raman measurements so far discussed, in order to achieve surface sensitivity and so that small changes in doping can be resolved (compared to using bulk graphite). In order to validate that our observations remain relevant for thicker graphitic layers such as the HOPG used for STM measurements, we performed similar measurements on bilayer graphene regions (produced by stacking two pieces of single-layer graphene[22]). We again observe no significant changes in the graphene peaks following oxygen-bubbling when only DCB is present, whilst with CuOEP dissolved in the DCB the G and 2D peak positions are seen to shift following O_2-bubbling confirming that a change in the interaction between CuOEP and graphitic surfaces is still seen. This change in molecule-substrate interaction resulting from oxidation of the CuOEP is therefore implicated in the distinctly different supramolecular assemblies observed by STM for CuOEP in DCB prior to and following O_2-bubbling.

4. Conclusion

We studied at the molecular level the adsorption and self-assembly of CuOEP and H_2OEP molecules on graphitic surfaces when dissolved in different solvents, and the effects of dissolved oxygen. Solvation effects on the self-assembly structure were clearly observed. Our results show that the Cu center of the CuOEP molecule plays an important role in the interaction with graphitic substrates. We have shown that dissolved molecular O_2 in DCB produces distinct changes in the molecular self-assembly of the molecules while no change is observed in DD due to the strong solvation effects of this solvent. Importantly no changes were observed on the H_2OEP molecules, confirming the activity of the Cu metal center in binding of O_2.

Complementary Raman spectroscopy revealed that the presence of oxygen within the DCB solution alters the molecule-substrate interaction, which we attribute to charge transfer from the graphitic substrate to facilitate oxygen adsorption on the Cu center of CuOEP. This same behavior was not observed with DD as the solvent, where the supramolecular assembly remains similar for H_2OEP and CuOEP whether molecular O_2 is dissolved in the solution or not.

Acknowledgements

This work was supported by the Office of Basic Energy Sciences (BES), Division of Materials Sciences and Engineering, of the U.S. Department of Energy (DOE) under Contract DE-AC02-05CH11231, through the Chemical and Mechanical Properties of Surfaces, Interfaces and Nanostructures program. R.S.W. acknowledges a Research Fellowship from St. John's College, Cambridge and a EU Marie Skłodowska-Curie Individual Fellowship (Global) under grant ARTIST (no. 656870) from the European Union's Horizon 2020 research and innovation programme. B.E. acknowledges the Early Postdoc Mobility fellowship from the Swiss National Research Funds (SNF).

References

[1] Foster, J. S.; Frommer, J. E. Imaging of Liquid Crystals Using a Tunneling Microscope. *Nature* **1988**, *339*, 542-545.

[2] Lehn, J.-M. Toward Complex Matter: Supramolecular Chemistry and Self-organization. *PNAS* **2002**, *99*, 4763-4768.

[3] Ramoino, L. Adsorption and Self-organization of CuOEP on Heterogeneous Surfaces: Tuning the Molecule-Substrate Interaction, Ph.D. Dissertation, University of Basel, Switzerland (2005).

[4] Seufert, K.; Bocquet, M.-L. Willi Auwärter, W.; Weber-Bargioni, A.; Reichert, J.; Lorente, N.; Barth, J. V. Cis-dicarbonyl Binding at Cobalt and Iron Porphyrins with Saddle-shape Conformation. *Nature Chem.*, **2011**, *3*, 14-119.

[5] Otsuki, J. STM Studies on Porhyrins. *Coord. Chem. Rev.* **2010**, *254*, 2311-2341.

[6] Auwärter, W.; Écija, D.; Klappenberger, F.; Barth, J. V. Porphyrins at Interfaces. *Nature Chem*. **2015**, *7*, 105-120.

[7] Ishihara, S.; Labuta, J.; Rossom, W. V.; Ishokawa, D.; Minami, K.; Hill, J. P.; Ariga, K. Porphyrin-based Sensor Nanoarchitectonics in Diverse Physical Detection Modes. *Phys. Chem. Chem. Phys.* **2014**, *16*, 9713-9746.

[8] Jeong, Y.-H.; Yoon, H.-J.; Jang, W.-D. Dendrimer Porphyrin-based self-assembled Nano-devices for Biomedical Applications. *Polym. J.*, **2012** *44*, 512-521.

[9] Walter, M. G.; Rudine, A. B.; Wamser, C. C. Porphyrins and Phthalocyanines in Solar Photovoltaic Cells. *J. Porphyrins Phthalpcyanines*, **2010** *14*, 759-792.

[10] Kadish, K. M.; Smith, K. M.; Guilard, R. The Porphyrin Handbook: Bioinorganic and bioorganic chemistry. Academic Press: San Diego, 1990; Vol. 11.

[11] Solomon, E. I.; Chen, P.; Metz, M.; Lee, S. K.; Palmer, A. E. Oxygen Binding, Activation, and Reduction to Water by Copper Proteins. *Angew. Chem. Int. Ed*. **2001** *40*, 4570-4590.

[12] Ogunrinde, A.; Hipps, K. W.; Scudiero, L. A Scanning Tunneling Microscopy Study of Self-Assembly Nickel(II) Octaethylpophyrin Deposited from Solution on HOPG. *Langmuir* **2006**, *22*, 5697-6701.

[13] Chen, Q.; Yan, H.; Yan, C.; Pan, G.; Wan, L.; Wen, G.; Zhang, D. STM Investigation of the Dependence of Alkane and Alkane Derivatives Self-assembly on Molecular Chemical Structure on HOPG Surface. *Surf. Sci.* **2008**, *602*, 1256-1266.

[14] Wang, H.; Wang, C.; Zeng, Q.; Xu, S.; Yin, S.; Xu, B.; Bai, C. Chain-length-adjusted Assembly of Substituted Porphyrins on Graphite. *Surf. Interface Anal.* **2001**, *32*, 266-270.

[15] Liu, A. Z.; Lei, S. B. Structure Dependent Packing Behavior of Phthalocyanine on the Surface of Graphite. *Surf. Interface Anal.* **2007**, *39*, 33-38.

[16] Miyake, Y.; Tanaka, H.; Ogawa, T. Scanning Tunneling Microscopy Investigation of Vanadyl and Cobalt (II) Octaethylporphyrin Self-Assembled Monolayer Arrays on Graphite. *Colloids and surfaces A: Physicochem. Eng. Aspects* **2008**, *313-314*, 230-233.

[17] Oncel, N.; Bernasek, S. L. The Effect of Molecule-Molecule and Molecule-Substrate Interaction in the Formation of Pt-Octaethyl Porphyrin Self-Assembled Monolayers. *Appl. Phys. Lett.* **2008**, *92*, 133305.

[18] Chilukuri, B.; Mazur, U.; Hipps, K. W. Effect of Dispersion on Surface Interactions of Cobalt(II) Octaethylporphyrin Monolayer on Au(111) and HOPG(0001) Substrates: A Comparative First Principles Study. *Phys. Chem. Chem. Phys.* **2014**, *16*, 14096-14107.

[19] Gruden-Pavlovíc, M.; Grubišiæ, S.; Zlatar, M.; Niketìc, S. R. Molecular Mechanics Study of Nickel(II) Octaethylporphyrin Adsorbed on Graphite(0001). *Int. J. Mol. Sci.* **2007**, *8*, 810-829.

[20] Friesen, B. A.; Bhattarai, A.; Mazur, U.; Hipps, K. W. Single Molecule Imaging of Oxygenation of Cobalt Octaethylporphyrin at the Solution/Solid Interface: Thermodynamics from Microscopy. *J. Am. Chem. Soc.* **2012**, *134*, 14897-14904.

[21] Hofmann, S.; Braeuninger-Weimer, P.; Weatherup, R. S. CVD-Enabled Graphene Manufacture and Technology. *J. Phys. Chem. Lett.* **2015**, *6*, 2714–2721.

[22] Weatherup, R. S.; Eren, B.; Hao, Y.; Bluhm, H.; Salmeron, M. B. Graphene Membranes for Atmospheric Pressure Photoelectron Spectroscopy. *J. Phys. Chem. Lett.* **2016**, *7*, 1622–1627.

[23] Kratzer, M.; Bayer, B. C.; Kidambi, P. R.; Matković, A.; Gajić, R.; Cabrero-, A.; Weatherup, R. S.; Hofmann, S.; Teichert, C. Effects of Polymethylmethacrylate-Transfer Residues on the Growth of Organic Semiconductor Molecules on Chemical Vapor Deposited Graphene. *Appl. Phys. Lett.* **2015**, *106*, 103101.

[24] Zou, Z.; Wei, L.; Chen, F.; Liu, Z.; Thamyongkit, P.; Loewe, R. S.; Lindsey, J. S.; Mohideen, U.; Bocian, D. F. Solution STM Images of Porphyrins om HOPG Reveal that Subtle Differences in Molecular Structure Dramatically Alter Packing Geometry. *J. Porphyrins Phthalocyanines* **2005**, *9*, 387-392.

[25] Zhang, X.; Xu, H.; Shen, Y.; Wang, Y.; Shen, Z.; Zeng, Q.; Wang, C. Solvent Dependent Supramolecular self-assembly and Reversal of a Modified Porphyrin. *Phys. Chem. Chem. Phys.*, **2013**, *15*, 12510-12515.

[26] Gopakumar, T. G.; Muller, F.; Hietschold, M. Scanning Tunneling Microscopy and Scanning Tunneling Spectroscopy Studies of Planar and Nonplanar Naphthalocyanines on Graphite (0001). Part 1: Effect of Nonplanarity on the Adlayer Structure and Voltage-induced Flipping of Nonplanar Tin−Naphthalocyanine. *J. Phys. Chem. B* **2006**, *110*, 6051-6059.

[27] den Boer, D.; Li, M.; Habets, T.; Iavicoli, P.; Rowan, A. E.; Nolte, R. J. M.; Speller, S.; Amabilino, D. B.; De Feyter, S.; Elemans, J. A. A. W. Detection of Different Oxidation States of Individual Manganese Porphyrins during Their Reaction with Oxygen at a Solid/liquid Interface. *Nat. Chem.* **2013**, *5* 621–627.

[28] Golovanov, I. B.; Zhenodarova, S. M. Quantitative Structure-Property Relationship: XXIII. Solubility of Oxygen in Organic Solvents. *Russ. J. Gen. Chem.* **2005**, *75*, 1879-1882.

[29] Jensen, K. P.; Ryde, U. How O2 Binds to Heme, *J. Biol. Chem.* **2004**, *279*, 14561-14569.

[30] D'Arsié, L.; Esconjauregui, S.; Weatherup, R.; Guo, Y.; Bhardwaj, S.; Centeno, A.; Zurutuza, A.; Cepek, C.; Robertson, J. Stability of Graphene Doping with MoO_3 and I_2. *Appl. Phys. Lett.* **2014**, *105*, 103103.

[31] Spaulding, L.; Chang, C. Resonance Raman Spectra of Metallooctaethylporphyrins. Structural Probe of Metal Displacement. *J. Am. Chem. Soc.* **1975**, *97*, 2517–2525.

Figures

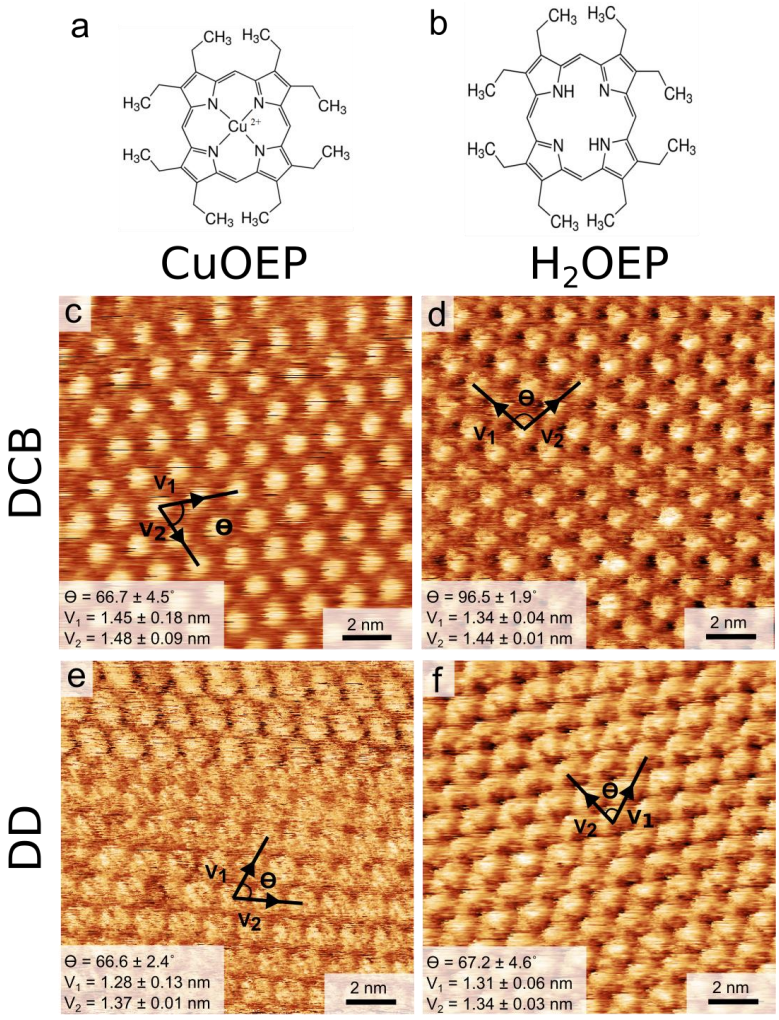

Figure 1 (a) and (b) are the molecular schemes of CuOEP and H_2OEP molecules, respectively. (c,d) STM images of CuOEP and H_2OEP supramolecular self-assemblies on the HOPG surface in equilibrium with molecules dissolved in a DCB solution (V_b = -0.9 V, I_t = 150 pA and V_b = -0.78 V, I_t = 100 pA, respectively). (e,f) STM images of CuOEP and H_2OEP supramolecular self-assemblies obtained using a DD solution instead of DCB (V_b = -1.2 V, I_t = 100 pA and V_b = -0.78 V, I_t = 20 pA, respectively). Lattice parameters of each supramolecular self-assembly is indicated in the corresponding image.

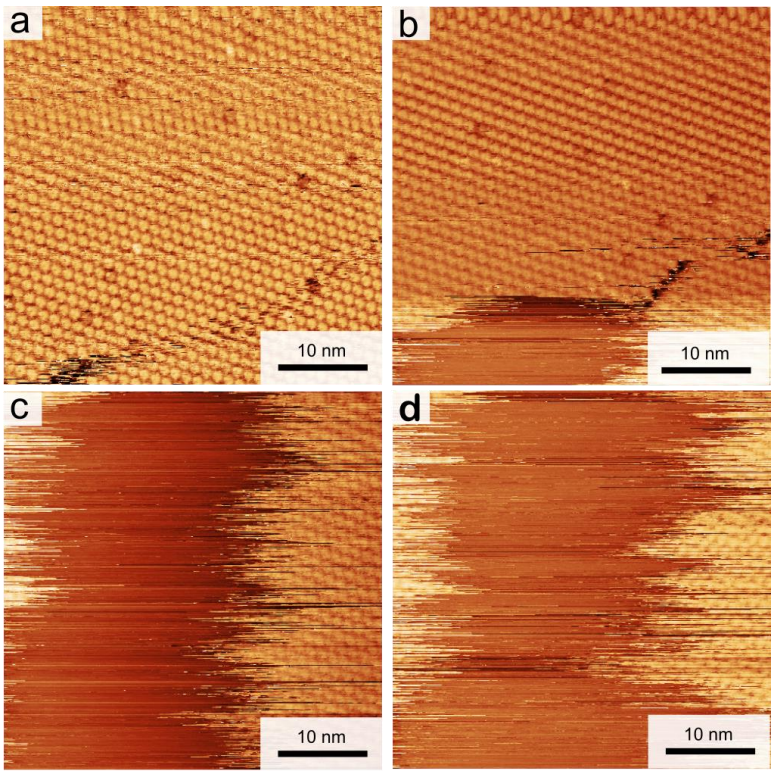

Figure 2 Time series STM images of CuOEP molecules in a DD solution assembled on HOPG (V_b = -1.2 V, I_t =100 pA). Time interval between images is around 2 minutes. Tip induced manipulation of CuOEP molecules results in their complete removal from the scanned area. The molecules pile up around the scanned frame.

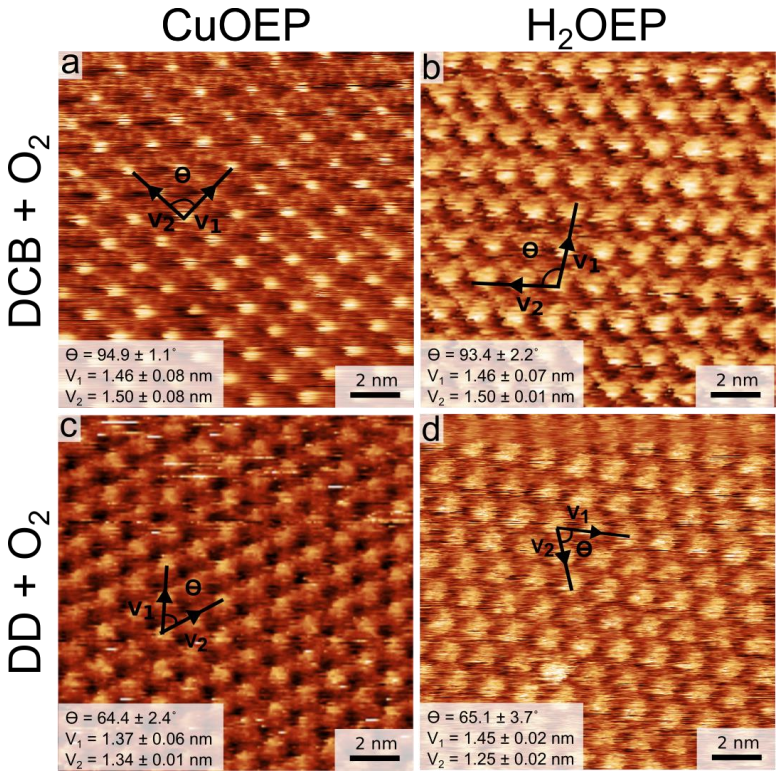

Figure 3 STM images of self-assembled layers of CuOEP and H_2OEP at DCB/HOPG interface and DD/HOPG interface after oxygen bubbling treatment of the solvents. Compare with the images in Figure 1c-f. (a) and (b) are respectively CuOEP and H_2OEP in DCB (V_b = -0.8 V, I_t = 55 pA; V_b = -0.78 V, I_t = 60 pA). (c) and (d) are respectively CuOEP and H_2OEP in DD (V_b = -1.2 V, I_t = 100 pA; V_b = -0.78 V, I_t = 40 pA). Lattice parameters of each supramolecular self-assembly are indicated in the corresponding images.

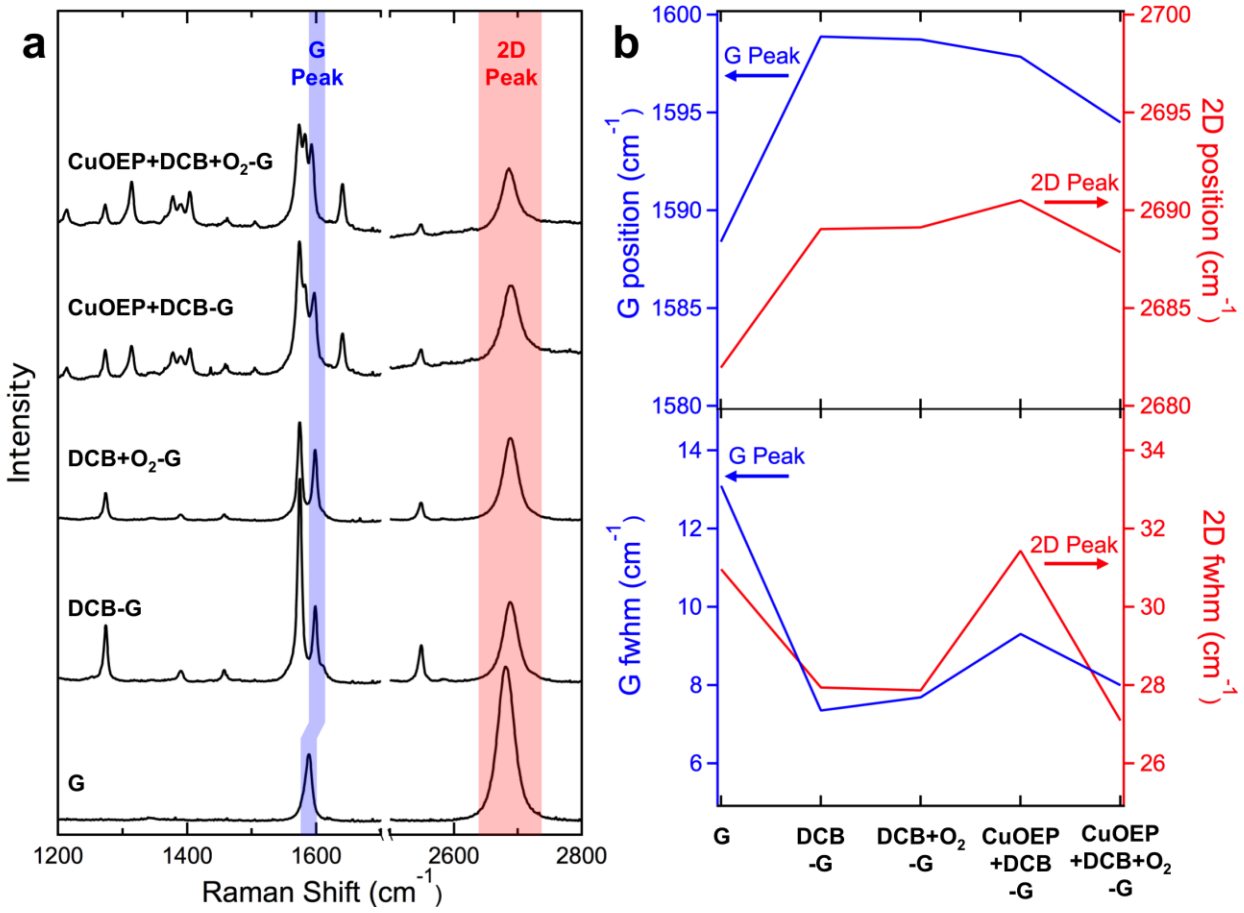

Figure 4 (a) Raman Spectra measured for CVD graphene [G] transferred onto SiO_2(300nm)/Si, with DCB [DCB-G], with O_2-bubbled DCB [DCB+O_2-G], with CuOEP dissolved in DCB [CuOEP+DCB-G], with CuOEP dissolved in O_2-bubbled DCB [CuOEP+DCB+O_2-G]. (b) G and 2D peak positions and widths (fwhm) obtained for these samples by fitting the peaks with single Lorentzian functions.